

## Boron-related minority-carrier trapping centers in *p*-type silicon

Daniel Macdonald,<sup>a)</sup> Mark Kerr, and Andrés Cuevas

*Department of Engineering and Faculty of Engineering and Information Technology,  
The Australian National University, Canberra ACT 0200, Australia*

(Received 28 April 1999; accepted for publication 14 July 1999)

Photoconductivity-based measurements of recombination lifetimes in multicrystalline silicon are often hampered by carrier trapping effects, which cause a characteristically large relative increase in the photoconductance. Single-crystal *p*-type float-zone wafers of varying resistivities were cross contaminated with multicrystalline wafers that exhibited such trapping. A proportion of the impurities present in the multicrystalline samples was found to effuse into the float-zone wafers, where they act as both recombination centers and trapping centers. By the application of a simple theoretical model, the trap density in the float-zone samples was determined, and found to be directly proportional to the boron-dopant concentration. These results suggest that the trapping centers are caused by boron-impurity pairs. © 1999 American Institute of Physics.

[S0003-6951(99)01537-5]

Trapping of minority carriers in multicrystalline silicon (mc-Si) and other materials is a well-known phenomenon, and has been observed by several authors.<sup>1–3</sup> In contrast to deep-lying recombination centers, the trapping centers (referred to below as traps), take the form of states within the energy gap that temporarily hold minority carriers, before releasing them back into the band. Despite the fact that such centers may not directly contribute to recombination, their impact on the photoconductivity of a sample can be dramatic, and if such measurements are used to determine recombination lifetimes, the results can be misleading.

In *p*-type silicon, charge neutrality considerations dictate that the presence of minority-carrier traps causes a relative increase in the concentration of holes (majority carriers) at carrier densities comparable to and below the trap density.<sup>4</sup> As a result, the photoconductivity is larger than would be the case when traps are absent, in turn resulting in a larger apparent lifetime. The unfortunate consequence is that recombination lifetime measurements at lower injection levels, which are often of practical interest, become difficult. In order to attempt to overcome these problems, it is desirable to know more about the physical cause of the trapping centers.

All lifetime measurements presented in this letter were performed using the quasi-steady-state photoconductance (QSSPC) technique, the practical application of which is described elsewhere.<sup>5</sup> Injection-level-dependent carrier mobilities were modeled after the data of Krausse<sup>6</sup> and Dannhauser.<sup>7</sup> Although the results presented here are steady state in nature, any photoconductance-based method, such as transient photoconductance decay (PCD), would be subject to the same trapping phenomena.<sup>1</sup> The QSSPC data analysis was performed with a recently improved approach,<sup>8</sup> allowing a large range of lifetimes to be measured. The instrument used had sufficiently low-noise levels to allow trap densities down to  $4 \times 10^{11} \text{ cm}^{-3}$  to be measured.

Figure 1 shows the results of QSSPC apparent lifetime data obtained from a *p*-type 1.0  $\Omega \text{ cm}$  cast mc-Si solar-grade

sample with a very high trap density. Surface passivation was achieved by a light phosphorus diffusion and oxidation as described below. The rapid increase in inverse apparent lifetime from low to high injection is due to the traps, and even at the highest injection level measured we cannot associate the apparent lifetime with the recombination lifetime. The low recombination lifetime in this sample necessitated the use of infrared light to provide uniform carrier profiles, which limited the maximum measurable injection level to  $7.0 \times 10^{15} \text{ cm}^{-3}$ .

A simple theoretical trapping model can be fitted to such experimental data, allowing the trap density  $N_t$  and the recombination lifetime  $\tau_r$  to be determined.<sup>9</sup> The mathematical development of the model under the QSSPC regime is given in a previous letter.<sup>3</sup> For the sample in Fig. 1, the trap density computed by this method is  $7 \times 10^{15} \text{ cm}^{-3}$ , with the recombination lifetime assumed constant and determined to be 0.7  $\mu\text{s}$ . Note that in this case the trap density is so high as to make a direct measurement of the recombination lifetime  $\tau_r$  impossible. However, by fitting the trapping model,  $\tau_r$  can be determined with reasonable accuracy.

In previous work, we have found that the trap density in mc-Si wafers decreases after phosphorus gettering, and that

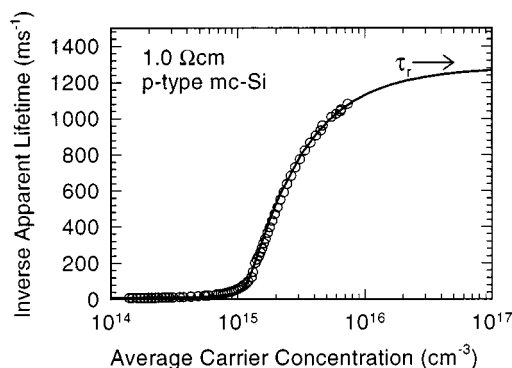


FIG. 1. Inverse apparent lifetime vs average carrier concentration for a 1.0  $\Omega \text{ cm}$  B-doped *p*-type mc-Si wafer. The open circles are experimental data, and the solid line the trapping model. Fitting the model yields a trap density of  $7.0 \times 10^{15} \text{ cm}^{-3}$  and a constant recombination lifetime  $\tau_r$  of 0.7  $\mu\text{s}$ .

<sup>a)</sup>Electronic mail: daniel@faceng.anu.edu.au

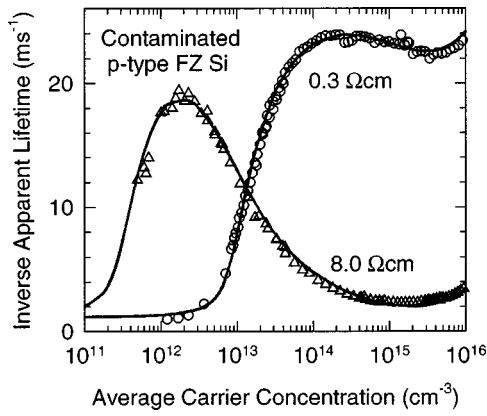


FIG. 2. Inverse apparent lifetime vs average carrier concentration for 0.3 and 8.0  $\Omega$  cm cross-contaminated FZ Si wafers. The open symbols are experimental data. The solid lines represent the trapping model fitted with the recombination lifetime  $\tau_r$ , modeled by two SRH centers and an emitter term. The apparent lifetime can only be associated with the recombination lifetime at carrier concentrations above  $1 \times 10^{14}$  and  $2 \times 10^{12}$   $\text{cm}^{-3}$  for the 0.3 and 8.0  $\Omega$  cm samples, respectively.

the remaining traps are correlated to the dislocation density.<sup>3</sup> In this letter, we investigate whether the traps present prior to gettering are related to mobile impurities in the mc-Si. Such impurities can be transferred to nearby high-quality, single-crystal float-zone (FZ) wafers by effusion at high temperature.<sup>10</sup> This cross contamination produces a reduction in the recombination lifetimes of the FZ wafers that is proportional to the initial contamination level in the mc-Si wafers. We have found that these contaminated FZ wafers also exhibit considerable trapping effects, which is a clear indication that mobile impurities can also be responsible for the creation of trapping centers. It is possible that the same type of impurity is responsible for both the increased recombination activity and the trapping centers, or alternatively, that more than one type of impurity could be present, some of which form deep recombination levels and others trapping states.

An important advantage of the cross-contamination experiments is that they allow the study of trapping and recombination centers in a material that is practically free of crystallographic defects. They also provide a way of examining the correlation between the background doping levels and the magnitude of the trapping effects by contaminating FZ wafers of different resistivities. This is generally not possible with mc-Si wafers, which come only in a narrow dopant density range, and in which a similar crystal quality cannot be guaranteed.

Cross contamination of *p*-type FZ Si wafers was achieved by an 840  $^{\circ}\text{C}$  light phosphorus diffusion followed by a thin thermal oxide growth at 900  $^{\circ}\text{C}$ , for a total of 60 min. The high temperature allows the effusion of impurities from the mc-Si to the FZ Si (separated by about 5 mm), while the diffusion and oxidation passivate the surfaces for lifetime measurements. To ensure measurable trapping effects in the FZ wafers, we used mc-Si samples with high trap densities (around  $7 \times 10^{15}$   $\text{cm}^{-3}$ ), similar to the sample presented in Fig. 1.

Figure 2 shows lifetime measurements of two such cross-contaminated FZ samples of 0.3 and 8.0  $\Omega$  cm resistivity. At higher injection levels the data reflect the recombina-

tion lifetimes, however, at around  $1 \times 10^{14}$  and  $2 \times 10^{12}$   $\text{cm}^{-3}$  for the 0.3 and 8.0  $\Omega$  cm samples, respectively, trapping effects begin to dominate. The presence of the contaminating species in the FZ material has two effects on lifetime—first, the introduction of minority-carrier traps and the associated increase in apparent lifetime at low injection, and second the introduction of recombination centers and the resulting Shockley–Read–Hall (SRH) dependence of the recombination lifetime on injection level.<sup>4,11</sup> The presence of the emitter caused by the phosphorus diffusion in these samples also impacts on the lifetime measurements at the highest injection levels.<sup>12</sup>

As well as in the experimental data, Fig. 2 also shows fit lines for the theoretical model. However, the fitting procedure is more complex than that used in Fig. 1, where the recombination lifetime  $\tau_r$  was assumed constant. The curves in Fig. 2 clearly show an injection-level dependence at carrier densities higher than the region where traps dominate. This is typical of SRH recombination centers, and also of emitter recombination, as mentioned above. As a result, for *p*-type Si,  $\tau_r$  must be modeled by<sup>4,12</sup>

$$\frac{1}{\tau_r} = \frac{1}{\tau_{\text{SRH}}} + \frac{1}{\tau_{\text{emit}}},$$

where

$$\frac{1}{\tau_{\text{SRH}}} = \frac{N_A + \Delta n}{\tau_{p0}(n_1 + \Delta n) + \tau_{n0}(N_A + p_1 + \Delta n)},$$

and

$$\frac{1}{\tau_{\text{emit}}} = \frac{2J_0(N_A + \Delta n)}{qn_i^2 W}.$$

Here,  $\Delta n$  is the excess carrier density,  $N_A$  the dopant density,  $n_1$  and  $p_1$  the equilibrium densities of electrons and holes, respectively, when the Fermi energy coincides with the flaw energy, and  $\tau_{n0}$  and  $\tau_{p0}$  the capture time constants for electrons and holes.<sup>4</sup>  $J_0$  is the emitter saturation current, which characterizes recombination in the diffused regions, and  $n_i$  and  $W$  the intrinsic carrier concentration and sample thickness, respectively. The values of  $J_0$  used in the fitting procedure were measured experimentally for each sample under high injection conditions,<sup>12</sup> and were typically  $5 \times 10^{-14}$   $\text{A cm}^{-2}$ .

To obtain an accurate fit to the experimental data in Fig. 2, it was necessary to model  $\tau_r$  with two SRH centers and an emitter term. Having two centers means that there are six fit parameters for the SRH contribution to  $\tau_r$ , resulting in a large number of possible sets of parameters that provide reasonable agreement. As a consequence, it is not possible to uniquely determine  $\tau_{n0}$  and  $\tau_{p0}$  or the energy level of the recombination centers from our experiments. However, for any of these sets of parameters that provide a good fit, the possible values of the trap density  $N_t$  are restricted to a narrow range. Hence, we are in a position to accurately specify  $N_t$ , even if we can infer little about the nature of the SRH centers.

Before moving on to discuss the cross-contamination results further, there is the important question of whether the effects observed in the contaminated FZ wafers are bulk or surface effects. At the surfaces there exist relatively highly

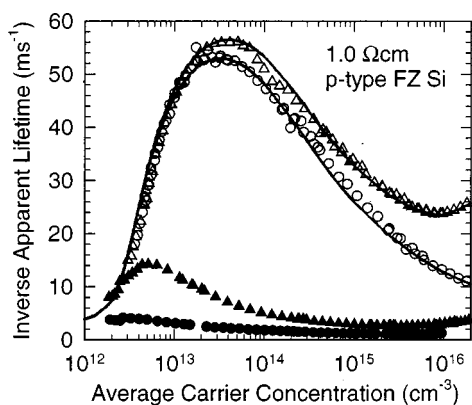


FIG. 3. Inverse apparent lifetime vs average carrier concentration for a contaminated 1.0  $\Omega$  cm FZ sample with emitter passivation (open triangles) and SiN passivation (open circles), and also for a clean 1.0  $\Omega$  cm FZ sample with emitter passivation (solid triangles) and SiN passivation (solid circles). The solid lines for the contaminated cases represent the trapping model fitted with two SRH centers and an emitter term.

doped phosphorus layers, in which impurities are in general highly soluble. Hence, it is conceivable that the impurities adsorbed onto the surfaces of the FZ wafers during cross contamination remain in the thin diffused regions. To determine if this was indeed the case, a contaminated 1.0  $\Omega$  cm sample was etched to remove the phosphorus layers. The sample was then repassivated with plasma-enhanced chemical-vapor deposition silicon nitride (SiN) films deposited at 400 °C, and the lifetimes remeasured. The results are depicted in Fig. 3.

The results for the emitter passivation and SiN passivation agree very well. There is a difference at higher injection levels, but this is due entirely to the presence of emitter recombination in the diffused sample, which is, of course, not present in the SiN-passivated sample. The trapping model with two SRH centers was fitted for both of these cases, with an emitter term also included for the diffused case. The fit shown for the SiN-passivated data is simply that for the diffused case with all trapping and SRH parameters the same, except with  $J_0=0$  (i.e., no emitter recombination).

Also shown on Fig. 3 are SiN-passivated and diffused 1.0  $\Omega$  cm samples that have not been cross contaminated. The fact that both these curves represent much higher apparent lifetimes at all injection levels strongly indicates that the results for the contaminated case reflect mainly bulk apparent lifetimes. The clean samples also show evidence of trapping, which may be related to the surfaces, but with much lower trap densities. Consequently, we are able to interpret the computed trap densities for the contaminated cases as relating to a volume concentration.

The bulk trap density was determined for a range of contaminated FZ wafers of resistivity from 0.3 to 1000  $\Omega$  cm. For the 1000  $\Omega$  cm case the trap density was so small ( $<1 \times 10^{11}$  cm<sup>-3</sup>) as to be unmeasurable. The results for the other wafers are shown in Fig. 4 as a function of boron concentration in the FZ substrate. There is a clear linear relationship between these two variables, implying that the traps are related to boron-impurity pairs. Multicrystalline samples with lower trap densities and higher recombination lifetimes (and hence, lower mobile impurity concentrations)

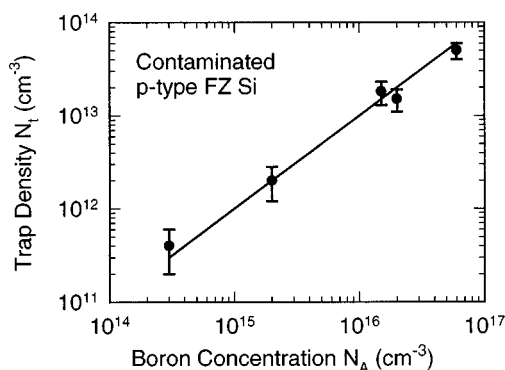


FIG. 4. Boron concentration  $N_A$  vs trap density  $N_t$  for cross-contaminated B-doped  $p$ -type FZ wafers of different resistivities. The error bars reflect uncertainty in the trap densities, which are determined by fits like those shown in Fig. 2. The solid line represents the linear fit  $N_t = 0.001 N_A$ .

than those used in the experiments above were also used to cross-contaminate 1  $\Omega$  cm FZ wafers. The corresponding trap densities in these FZ wafers were lower than for the heavily contaminated FZ wafers, indicating a relationship between trap density and mobile impurity concentration qualitatively similar to that in Fig. 4. The impurities responsible for the trapping centers have clearly come from the mc-Si, and hence, must be highly mobile in silicon at high temperatures in order to effuse effectively. Prime candidates for such an impurity are transition metals.

As mentioned, previous work has revealed that the trap density in gettered mc-Si wafers is related to the dislocation density in the material. In view of the results presented here, this suggests that there are two sources of trapping centers present, first boron-impurity pairs, which can be removed by gettering, and second dislocation-related centers that cannot.

In conclusion, cross contamination of FZ wafers with mc-Si wafers reveals that the impurities causing trapping centers in the mc-Si are mobile and can penetrate the bulk of the FZ wafers. It seems reasonable, therefore, to associate these traps with highly mobile impurities such as transition metals. Moreover, the density of such traps is linearly related to the boron concentration in the  $p$ -type FZ substrates, implicating boron-impurity pairs.

Thanks to Eurosolare SpA for supplying the mc-Si wafers and to Jan Schmidt for fruitful discussions. This work has been supported by the Australian Research Council.

- <sup>1</sup>R. K. Ahrenkiel and S. Johnson, *Sol. Energy Mater. Sol. Cells* **55**, 59 (1998).
- <sup>2</sup>A. Romanowski, A. Buczkowski, A. Karoui, and G. Rozgonyi, *8th Workshop on Crystalline Silicon Solar Cell Material and Processing*, Copper Mountain, Colorado (NREL) Golden, CO (1998), p. 196.
- <sup>3</sup>D. Macdonald and A. Cuevas, *Appl. Phys. Lett.* **74**, 1710 (1999).
- <sup>4</sup>R. A. Smith, *Semiconductors* (Cambridge University Press, Cambridge, 1959).
- <sup>5</sup>R. A. Sinton and A. Cuevas, *Appl. Phys. Lett.* **69**, 2510 (1996).
- <sup>6</sup>J. Krausse, *Solid-State Electron.* **15**, 1377 (1972).
- <sup>7</sup>F. Dannhauser, *Solid-State Electron.* **15**, 1371 (1972).
- <sup>8</sup>H. Nagel, C. Berge, and A. Aberle, *J. Appl. Phys.* (submitted).
- <sup>9</sup>J. A. Hornbeck and J. R. Haynes, *Phys. Rev.* **97**, 311 (1955).
- <sup>10</sup>D. Macdonald and A. Cuevas, *2nd World Conference on Photovoltaic Solar Energy Conversion*, Vienna (European Commission, Ispra, Italy, 1998), p. 2418.
- <sup>11</sup>W. Shockley and W. T. Read, *Phys. Rev.* **87**, 835 (1952).
- <sup>12</sup>A. Cuevas, *Sol. Energy Mater. Sol. Cells* **57**, 277 (1999).